

# Critical viscoelastic behavior of polydimethylsiloxane networks around the sol-gel threshold

Jennifer Gasparoux, Thomas Tixier, and Philippe Tordjeman\*

Laboratoire d'Analyse des Interfaces et de Nanophysique, UMR-5011, Université Montpellier II, CC082, Place E. Bataillon, 34095 Montpellier Cedex 5, France

(Received 14 September 2006; published 18 January 2007)

Seven model polydimethylsiloxane (PDMS) networks were obtained by hydrosilation of a difunctional vinyl-terminated PDMS prepolymer with a SiH-containing cross-linker. Viscoelastic experiments, completed by size exclusion chromatography and static light scattering experiments, were performed in order to study the influence of molecular parameters on the dynamic properties around the sol-gel threshold. The dynamic critical parameter  $u$  was determined from experiments close to and above the sol-gel threshold. Our results show that the growth mechanism of PDMS clusters and the viscoelastic behavior are a function of the ratio  $N/N_e$ , where  $N$  and  $N_e$  are, respectively, the numbers of Kuhn monomers between branch points and between entanglements. For  $N/N_e < 1$ , the growth mechanism of clusters is the critical percolation and  $u=0.69$ , and for  $N/N_e > 1$ , the growth mechanism of clusters is the diffusion-limited cluster aggregation and  $u=0.76$ .

DOI: [10.1103/PhysRevE.75.011802](https://doi.org/10.1103/PhysRevE.75.011802)

PACS number(s): 82.35.Lr, 83.80.Jx

## I. INTRODUCTION

The static properties of polymer networks around the sol-gel transition obey power laws where the critical exponent values are characteristic of the mechanism of connectivity [1–3]. A universality class is defined by a group of critical exponents, independent of the chemical structure, calculated in the framework of a theory of gelation. There are two main universality classes for the sol-gel transition. The first one, called the critical percolation class, describes the gelation of colloids, the polymerization of small multifunctional monomers, and the cross-linking of longer chains in solution [4–7]. The second one, called the mean field class, modeled by the Flory-Stockmayer theory [8–10], describes the vulcanization and cross-linking of long polymer chains [1,2,11]. The crossover between the two classes is given by the Ginzburg argument, which considers that the mean field theory describes well the molecular structure only if fluctuations of the order parameter in a correlation volume are negligible. Conversely, if fluctuations predominate, the molecular structure is completely described by the critical percolation theory. The literature shows that the experimental static properties of a majority of percolating systems depend on the experimental conditions like the solvent concentration [12,13] and are in agreement with either the critical percolation theory or the mean field theory [1,14]. On the other hand, the dynamic properties and particularly the viscoelastic properties of branched polymers around the gel point are not well understood. Experimental results show that the dynamic exponent  $u$  that characterizes the frequency dependence of the complex shear modulus seems to be nonuniversal and dependent on the chemical structure of the branched polymers. Most authors tried to link the viscoelastic properties, particularly the  $u$  values, to universality classes. However, we have to consider that the experimental critical viscoelastic properties are limited in frequency and the  $u$  values are characteristic of the dynamic of finite clusters or part of in-

finite clusters. Indeed, even if the final connectivity mechanism at the gel point should occur by critical percolation, one can observe different viscoelastic behaviors characterizing the dynamic of clusters or parts of clusters, which grew by mechanisms different from critical percolation. Recently, Rottureau *et al.* [15,16] showed that a finite or infinite cluster could be characterized by different fractal dimensions at different spatial scales, which should correspond to different  $u$  measured in different frequency ranges. It is clear that transitions in dynamic behavior of clusters associated with the transitions of growth mechanisms depend on the structural parameters of precursors and gelation conditions. Lusignan *et al.* [17] show that the dynamic exponent of random branched polyesters is a function of the ratio  $N/N_e$ , where  $N$  and  $N_e$  are, respectively, the numbers of Kuhn monomers between the branch points and between entanglements. For  $N/N_e < 2$ ,  $u$  is universal and is forecast by the Rouse fractal model ( $u=0.67$ ); the static properties are characteristic of the critical percolation class. For  $N/N_e > 2$ ,  $u$  is nonuniversal and is a decreasing function of the number of entanglements between branch points. In this case, the molecular structure of the network is predicted by the mean field theory.

We will present in this paper the viscoelastic properties around the gel point of two polydimethylsiloxane (PDMS) networks. These results complete those of a structural series of PDMS previously published in Refs [18,19]. Based on static light scattering and size exclusion chromatography experiments, we will show how the set of data yields a unified understanding of the static and dynamic properties of PDMS networks around the sol-gel transition. The paper is organized as follows: in Sec. III, we recall the background theory used to analyze the molecular structure and the viscoelastic properties of our PDMS networks. In Sec. III, we describe the chemical structure of our prepolymers and cross-linkers, the reaction conditions, and the experimental procedure of the molecular analysis and viscoelastic measurements. In Sec. IV, we present and discuss the experimental results. Section V is our conclusion.

\*Electronic address: [philippe.tordjeman@univ-montp2.fr](mailto:philippe.tordjeman@univ-montp2.fr)

## II. BACKGROUND THEORY

The scaling relations of both mean-field (vulcanization) and critical percolation classes present the same form, but differ in their exponent values [7]. Near the gelation threshold, polymer clusters are fractal with a mass scaling as a power of their radius  $R$ :  $M \propto R^{D_f}$ , where  $D_f$  is the fractal dimension of the clusters. The number of clusters of  $N$  Kuhn segments,  $n(N)$ , also obeys a scaling relation

$$n(N) \propto N^{-\tau} f\left(\frac{N}{N^*}\right), \quad (1)$$

where  $f(N/N^*)$  is the cutoff function that cuts off the power law at a characteristic large number of Kuhn segments,  $N^*$ . The number of Kuhn segments,  $N$ , is given by the relation

$$N = \frac{n_0 M}{m_0 C_\infty}, \quad (2)$$

where  $n_0$  is the number of main chain bonds per monomer,  $m_0$  the monomer molar mass,  $C_\infty$  the Flory characteristic ratio, and  $M$  the molecular weight of the polymer.

In the three-dimensional critical percolation, the theoretical fractal dimension is  $D_f=2.52$  and the overlap function is  $\phi(N) \approx 1$ . This function is equal to the total hard sphere volume fraction occupied by chains of size  $N$  and sections of larger chains of size  $N$  [20,21]. In this case, the excluded volume interaction is partially screened and the relation between  $D_f$  and the space dimension  $d$  is given by the hyper-scaling law

$$D_f(\tau - 1) = d.$$

On the other hand, in the three-dimensional mean-field theory  $D_f=4$  and  $\phi(N) \gg 1$ ; then, the excluded volume interaction is totally screened [7].

For the chemical gelation of polymers, the degree of connectivity of clusters is a function of the extent of reaction. If  $p$  is the fraction of reacted bonds and  $p_c$  its value at the gel point, the relative distance to the threshold is

$$\epsilon = \left| \frac{p - p_c}{p_c} \right|.$$

As the reaction proceeds, the polymers reach the gel point. Around the threshold, the static properties are quite well predicted by the critical percolation theory. Far below the threshold, the structural properties are modeled by the mean field theory. The relative distance to the threshold,  $\epsilon_G$ , which defines the crossover between the two theories is given by the Ginzburg criterion.  $\epsilon_G$  corresponds to the  $\epsilon$  value at which the largest polymers start overlapping significantly. de Gennes [22] showed that  $\epsilon_G$  scales as  $\epsilon_G \propto N^{-1/3}$ .

During the sol-gel transition, the viscoelastic properties of the material are function of  $\epsilon$ : for  $p < p_c$ , the polymer is a viscoelastic liquid characterized by a zero-frequency viscosity  $\eta$ , which diverges as one approaches the threshold:  $\eta \propto \epsilon^{-s}$ . On the contrary, for  $p > p_c$ , the polymer is a viscoelastic solid with a zero-frequency elastic modulus  $G$ , which increases above the gel point:  $G \propto \epsilon^t$ .

The zero-frequency properties are related to the low-frequency dependence of the complex modulus  $G^*(\omega)$ :

$$\eta = \lim_{\omega \rightarrow 0} \frac{G^*(\omega)}{i\omega}$$

and

$$G = \lim_{\omega \rightarrow 0} G^*(\omega).$$

At the sol-gel transition, the complex modulus follows a power law  $G' \propto G'' \propto \omega^u$  [23–25]. The relation between the dynamic exponent  $u$  and the zero-frequency exponents  $s$  and  $t$  is obtained from the scaling law

$$u = \frac{t}{s+t}. \quad (3)$$

Near the threshold, the dynamic behavior is governed by  $\omega^*$ , the frequency characteristic of the relaxation of the largest cluster  $N^*$ ; then, the complex modulus can be expressed by the general equation [24,26,27]

$$G^* = G_0 \epsilon^d f(i\omega/\omega^*),$$

with  $\omega^* = \omega_0 \epsilon^{s+t}$  and  $f(i\omega/\omega^*) \propto \omega^u$ . This relation is valid only below the characteristic cutoff frequency  $\omega_0$ . One can note that  $G'$  and  $G''$  are independent of  $\epsilon$  for  $\omega_0 > \omega > \omega^*$ , which is an important consequence of the self-similarity of the viscoelastic behavior. The storage and the loss modulus can be expressed by considering that the dynamics of a nonentangled fractal polymer melt can be represented by a Rouse bead-spring model. We assume that fractal polymers submit to a self-similar Brownian motion for which the diffusion coefficient scales as  $D \propto R^{-\beta}$ , where  $R$  is the radius of the fractal polymer and  $\beta$  is an exponent linked to the fractal dimension of the macromolecules. Following the Rouse approach, the stress is the sum of displacement contributions of all the springs and can be expressed as a simple function of the normal mode  $X_p$ :  $\sigma = \sum_p \sigma_p^c \langle X_p X_p \rangle$ , where  $\sigma_p^c$  is a constant proportional to the temperature.  $X_p$  is obtained from the Langevin equation for which the Brownian force is entropic. According to the Rouse approach,  $X_p$  takes an exponential form,  $X_p = X_p^0 \exp(-t/\tau_p)$ . The relaxation time  $\tau_p$  of the eigenmodes can be calculated independently by considering the Brownian motion of a single fractal cluster for which its Brownian relaxation time is given by the classical expression  $\tau_R \approx \frac{R^2}{D}$ , where  $R$  is the radius of the cluster and  $D$  its diffusion coefficient. One can express the relaxation time of the mode  $p$  as a function of  $\tau_R$ :  $\tau_p \approx p^{-1/u} \tau_R$ , with  $1 \leq p \leq m$ ,  $m$  being the longest relaxation mode depending on the molecular weight of the polymer. Following Martin *et al.* [28,29], the exponent  $u$  can be determined from the cluster diffusion coefficient  $D \approx R^{-\beta}$  by considering that the shortest relaxation time should be independent of the cluster size and of the mode  $m$ :  $\tau_m \approx m^{-1/u} \tau_R \approx m^0$ . In this model,  $m$  scales as  $m \propto R^{D_f}$ , where  $D_f$  is the fractal dimension of the polymer. Finally, we can write

$$\tau_p = \left(\frac{p}{m}\right)^{-(2+\beta)/D_f} \tau_0 = \left(\frac{p}{m}\right)^{-1/u} \tau_0, \quad (4)$$

where  $\tau_0$  is the relaxation time of the fastest mode that corresponds to the relaxation time of the smallest fractal cluster ( $\tau_0 \approx 1/\omega_0$ ). The  $\beta$  exponent depends on the molecular weight distribution of the polymer:  $\beta = D_f$  for monodisperse fractal polymers and  $\beta = \frac{D_f}{d}(2 + D_f) - 2$  for polydisperse fractal polymers [30,31].

The viscoelastic behavior of a branched polymer can be modeled by assuming that all the springs have a same elastic modulus  $G_c$ . Then, the storage and loss moduli can be expressed by

$$G'(\omega) = G_\infty(\omega\tau_0)^u \frac{u\pi}{2 \sin\left(\frac{u\pi}{2}\right)}, \quad (5)$$

$$G''(\omega) = G_\infty(\omega\tau_0)^u \frac{u\pi}{2 \cos\left(\frac{u\pi}{2}\right)}, \quad (6)$$

where  $G_\infty = mG_c$  for a monodisperse fractal polymer and  $G_\infty = mG_c A(\tau)$  for a polydisperse fractal polymer.  $A(\tau)$  is an unknown function, which is indicative of the molecular weight distribution. The expression of the loss angle,  $\delta = \arctan\left(\frac{G''}{G'}\right) = \frac{u\pi}{2}$ , is in agreement with experimental results. Chambon and Winter [32] have observed that  $G'(\omega) \equiv G''(\omega)$  for  $u=0.5$  and  $G'' > G'$  when  $u > 0.5$ , in agreement with the previous relations (5) and (6). To summarize, the fractal Rouse model enables one to determine the relation between the frequency exponent  $u$  and the fractal dimension  $D_f$ : for monodisperse fractal polymers,  $u$  is given by

$$u = \frac{D_f}{D_f + 2}, \quad (7)$$

where  $D_f$  is the fractal dimension of the polymer with fully screened hydrodynamic interactions. For polydisperse fractal polymers,  $u$  is given by

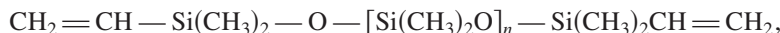
$$u = \frac{d}{D_f + 2}, \quad (8)$$

where  $d$  is the space dimension [30,31,33].

### III. EXPERIMENT

#### A. Chemical synthesis

The PDMS networks of cross-linked polymers used in this study are obtained by reaction between a vinyl-terminated linear polydimethylsiloxane prepolymer and a cross-linker containing SiH functions. The cross-linker is either a tetrakis(dimethylsiloxy)silane (TDS), a copolymer poly(dimethylsiloxane-co-methylhydrogenosiloxane), or a octakis(dimethylsilyloxy)silsesquioxane (ODS). These reagents were obtained from Gelest and were used as received. The chemical structure and the functionality of the prepolymers and cross-linkers were determined by  $^{29}\text{Si}$  and  $^1\text{H}$  NMR in  $\text{CDCl}_3$  with a Bruker Avance DPX 200 spectrometer. For  $^{29}\text{Si}$  NMR spectra,  $\text{Cr}(\text{Acac})_3$  was added as a relaxation reagent and gated decoupling, with a  $45^\circ$  flip angle and a 5-s recycle delay, was used as described by Williams *et al.* [34] for obtaining quantitative data. Seven PDMS networks were prepared from different starting products; we had at our disposal two vinyl-terminated PDMS prepolymers and six SiH cross-linkers of different functionalities and molecular weights. The first vinyl-terminated PDMS called prepolymer A has the following structure:



with  $n = 114 \pm 10$ .

The second vinyl-terminated PDMS called prepolymer B has the same chemical structure as prepolymer A but with  $n = 200 \pm 20$ .

Cross-linker 1 (TDS) is a four-functional silane cross-linker with the following structure:



Cross-linker 2 is a SiH-containing random copolymer with a mean functionality of 5:

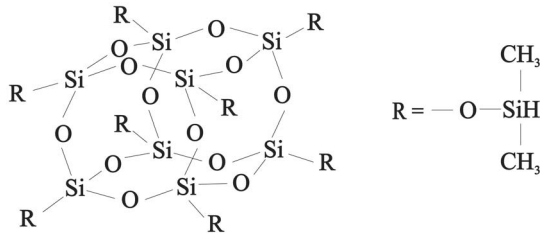


with  $x = 5 \pm 1$  and  $y = 24 \pm 3$ .

Cross-linkers 3, 4, and 5 have the same chemical structure as cross-linker 2 but with a functionality of 11 with  $x = 11 \pm 1$  and  $y = 24 \pm 3$  for cross-linker 3, a functionality of 7

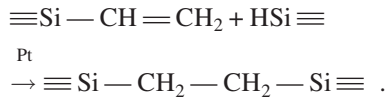
with  $x = 7 \pm 1$  and  $y = 100 \pm 10$  for cross-linker 4, and a functionality of 8 with  $x = 8 \pm 1$  and  $y = 8 \pm 1$  for cross-linker 5.

The cross-linker 6 (ODS) is an eight-functional cross-linker with the following structure:



Selected characteristics of the reagents are summarized in Table I

The cross-linking was performed in bulk by hydrosilylation with a platinum catalyst (solution of platinum in divinyltetramethyldisiloxane) [35,36]:



The reacted components of the seven PDMS networks, called polymers 1, 2, 3, 4, 5, 6, and 7, are presented in Table I. For all samples, 0.5  $\mu\text{l}$  of catalyst was introduced in 6 g of a blend of prepolymers and cross-linkers. In all cases, the concentration of the vinyl functions originating from the catalyst was negligible (at least 140 times lower than the concentration of vinyl originating from the prepolymers). The composition of the starting mixture is defined by the stoichiometric ratio  $r$  equal to the ratio of the concentration of initial silane functions to the one of initial vinyl functions:

$$r = \frac{[\text{SiH}]_0}{[\text{C}_2\text{H}_3]_0} = \frac{m_{\text{SiH}} f_{\text{SiH}} M_{\text{vinyl}}}{m_{\text{vinyl}} f_{\text{vinyl}} M_{\text{SiH}}} \quad (9)$$

Here SiH and *vinyl* subscripts refer, respectively, to the SiH-containing cross-linkers and the vinyl prepolymer.  $f$ ,  $m$ , and  $M$  are the functionality, the weight, and the number average molecular weight of the reagents.  $f$  and  $M$  were derived from NMR data;  $m$  was measured using a high-sensitivity balance ( $10^{-4}$  g).

Several samples were prepared for different  $r$  ratios less than 1 in order to determine the critical stoichiometric ratio

$r_c$  corresponding to the sol-gel transition. The experimental procedure consists in a first step to blend the prepolymer and the cross-linker for a given ratio  $r$ . Then, the catalyst is added under stirring and the cross-linking reaction begins. Prior to viscoelastic measurements, the samples are sonicated to eliminate bubbles.

## B. Rheology

The viscoelastic measurements were performed at a temperature of  $21 \pm 0.5$  °C using Rheometrics ARES and RFS III rheometers with parallel-disk geometry. These rheometers have transducers of 2000 g cm and 100 g cm allowing measurements of moduli above about 1 Pa and 0.1 Pa, respectively. Measurements were conducted in two stages. In the first stage, the evolution of  $G'$  and  $G''$  during the cross-linking reaction was measured at 10 rad/s for various  $r$  values. After 48 h at room temperature, the reaction is usually completed ( $G'$  and  $G''$  constant in time), which is confirmed by the disappearance of the resonance corresponding to SiH hydrogen atoms in the  $^1\text{H}$  NMR spectra of the samples. In the second stage, after completion of the cross-linking, the dynamic properties of the samples were measured. The frequency domain investigated is  $10^{-3}$ – $10^2$  rad/s. The critical stoichiometric ratio  $r_c$ , corresponding to the gelation threshold, is the value for which both  $G'$  and  $G''$  obey the power law  $\omega^u$ . Each dynamic curve was analyzed as a function of the relative distance from the threshold [19,27]:

$$\epsilon = \frac{r - r_c}{r_c} \quad (10)$$

Above the gel point, the zero-frequency modulus  $G$  and the crossover frequency value  $\omega^*$ , defined as the frequency where  $G'(\omega^*) = G''(\omega^*)$ , are obtained.

The curves  $G \propto \omega^{*u}$  allow one to verify the  $u$  values measured at  $r_c$ .

TABLE I. Starting products of the seven model PDMS networks called polymers 1–7, characterized by the number average molecular weight  $M_n$  (g/mol), the functionality  $f$ , and the density  $\rho$  of prepolymers and cross-linkers.  $M_n$  and  $f$  are determined by NMR, except for cross-linkers 1 and 6 (calculated from the chemical formula).

	Cross-linker 1	Cross-linker 2	Cross-linker 3	Cross-linker 4	Cross-linker 5	Cross-linker 6
	$M_n = 328.73$	$M_n = 2250 \pm 250$	$M_n = 2600 \pm 300$	$M_n = 6500 \pm 600$	$M_n = 1300 \pm 150$	$M_n = 1018$
	$f = 4$	$f = 5 \pm 1$	$f = 11 \pm 1$	$f = 7 \pm 1$	$f = 8 \pm 1$	$f = 8$
Reactants	$\rho = 0.886$	$\rho = 0.970$	$\rho = 0.980$	$\rho = 0.970$	$\rho = 0.970$	$\rho = 0.970$
Prepolymer A						
$M_n = 8600 \pm 700$	Polymer 1	Polymer 2	Polymer 3	Polymer 4	Polymer 5	Polymer 6
$f = 2$						
$\rho = 0.970$						
Prepolymer B						
$M_n = 15000 \pm 1400$		Polymer 7				
$f = 2$						
$\rho = 0.970$						

### C. Size exclusion chromatography

In order to characterize the molecular weight distribution of polymers around  $r_c$  and to measure the polydispersity exponent  $\tau$ , we used a classical analytical SEC apparatus with eluant THF. Two PL-gel columns (Polymer laboratories, type *E* and mixed *B*) were used in series. We removed the filter and the precolumn that usually protect the columns against pollution to decrease shear induced degradation of large molecular weight branched macromolecules. This method is discussed in the literature [37,38]. The chromatograms, shown in the figures below, were obtained using a concentration of  $1 \text{ mg/cm}^3$  and a flow rate of  $0.5 \text{ ml/min}$  for polymers synthesized just below  $r_c$ . At  $0.5 \text{ ml/min}$ , some degradation still occurs, but only for very large macromolecules beyond the resolution of the columns. The concentration of PDMS was monitored by a differential refractometer (R410 from Millipore-Waters) and was given in PS equivalent molecular weight ( $dn/dC=0.19 \text{ ml/g}$ ). The relation between the concentration  $C$  and the molecular weight  $M$  for a polymer around the sol-gel transition is [39]

$$C \propto M^{2-\tau} f\left(\frac{M}{M^*}\right), \quad (11)$$

for  $M_0 \leq M \leq M^*$  where  $M_0$  and  $M^*$  are, respectively, the low and high cutoff molecular weights. For  $\tau > 2$ , the maximum concentration does not depend on  $M^*$  and corresponds to the value of  $M_0$ . The experimental molecular distribution can be fitted by the following analytical expression [39]:

$$C = C_{max} \left(\frac{M}{M_0}\right)^{2-\tau} \exp\left(-\frac{M}{M^*}\right)^\beta, \quad (12)$$

where  $M^*$ ,  $M_0$ , and  $C_{max}$  are obtained from the chromatograms. The fits between experiments and Eq. (12) show that the more suitable value for  $\beta$  is 3.

### D. Static light scattering

In order to measure the swollen fractal dimension  $D_f^s$  of polymers around the gel point, static light scattering measurements were made at  $23^\circ \text{C}$  using an ALV-5000 multibit and multi- $\tau$  correlator with a Spectra Physics argon ion laser operating with vertically polarized light (wave length  $\lambda = 532 \text{ nm}$ ). They were done over a range of scattering angles  $10^\circ \leq \theta \leq 140^\circ$ . The corresponding range of the scattering wave vectors,  $q = (4\pi n_s / \lambda) \sin(\theta/2)$ , with  $n_s$  the solvent refractive index, is between  $2 \times 10^{-3}$  and  $4 \times 10^{-2} \text{ nm}^{-1}$ . Samples were synthesized just below  $r_c$  and then diluted 2000 times in toluene. The scattering intensity per unit volume  $I(q)$  was normalized by the intensity scattered by toluene at  $90^\circ$ . The effective fractal dimension  $D_f^{eff}$  is measured from the log-log plot of  $I(q)$ :  $I(q) \propto q^{D_f^{eff}}$ .  $D_f^{eff}$  depends on  $D_f^s$  and on the molecular distribution if  $2 < \tau < 3$ :  $D_f^{eff} = (3-\tau)D_f^s$ . On the other hand,  $D_f^{eff} = D_f^s$  if  $\tau \leq 2$  or  $\tau \geq 3$  [40,41]. The previous relations show that the  $\tau$  exponent has to be measured for each system before scattering light experiments.

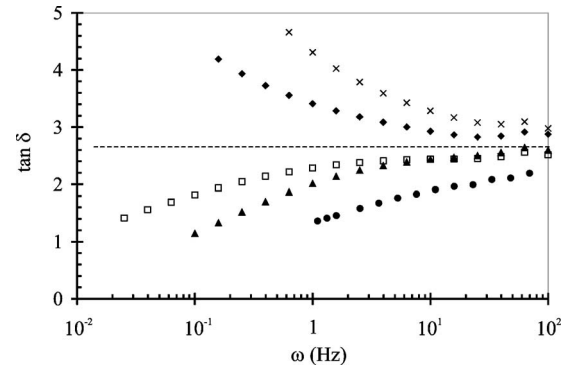


FIG. 1. Frequency dependence of  $\tan(\delta)$  of five polymer-5 gels, all synthesized at  $r \approx r_c = 0.25 \pm 0.01$ . The line corresponds to the mean value of  $\tan(\delta)$  leading to  $u_5 = 0.76 \pm 0.03$ .

## IV. RESULTS AND DISCUSSION

The viscoelastic properties at the sol-gel threshold for polymers 1, 2, 3, 4, and 7 are presented in Refs. [18,19]. The critical stoichiometric ratio for polymer 1 is  $r_{c1} = 0.44 \pm 0.01$ . The slope of the curves  $G'(\omega)$  and  $G''(\omega)$  and the frequency-independent value of the phase angle [ $\delta = \arctan(G''/G') = \frac{u_1 \pi}{2}$ ] give the critical exponent  $u_1 = 0.69 \pm 0.01$ . Similar results were obtained for polymers 2, 3, 4, and 7: we found  $r_{c2} = 0.26 \pm 0.01$ ,  $r_{c3} = 0.23 \pm 0.01$ ,  $r_{c4} = 0.30 \pm 0.01$ , and  $r_{c7} = 0.29 \pm 0.01$  and  $u_2 = 0.76 \pm 0.01$ ,  $u_3 = 0.75 \pm 0.03$ ,  $u_4 = 0.77 \pm 0.01$ , and  $u_7 = 0.76 \pm 0.01$ .

In the case of the new polymer 5, we were not able to measure the viscoelastic behavior at the sol-gel threshold. Due to the very high functionality of the cross-linkers ( $f=8$ ), a very small variation of the  $r$  value induces a large change in the viscoelastic behavior. Actually, our experimental precision on  $r$  is not high enough to prepare a sample with  $r$  exactly equal to  $r_c$ . Nevertheless,  $r_c$  were estimated from the rheological curves for which  $\tan(\delta)$  is nearly constant for the largest frequency domain:  $r_{c5} = 0.25 \pm 0.01$ . The  $u$  exponent was obtained from the asymptotic value of  $\tan(\delta)$  at high frequency; the resulting exponent is  $u_5 = 0.76 \pm 0.03$  (Fig. 1).

The critical ratio of polymer 6 is  $r_{c6} = 0.21 \pm 0.01$ . Its critical viscoelastic behavior is shown in Fig. 2 and is characterized by  $u_6 = 0.77 \pm 0.01$ .

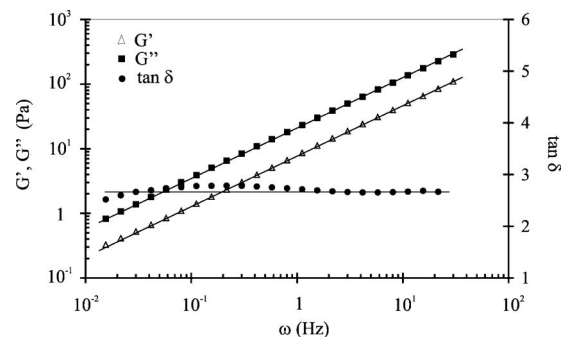


FIG. 2. Power law viscoelastic behavior and  $\tan(\delta)$  of polymer 6 at the gelation threshold. The slope of the log-log curves of the frequency dependence of  $G'$  and  $G''$  is  $u_6 = 0.76 \pm 0.01$ .

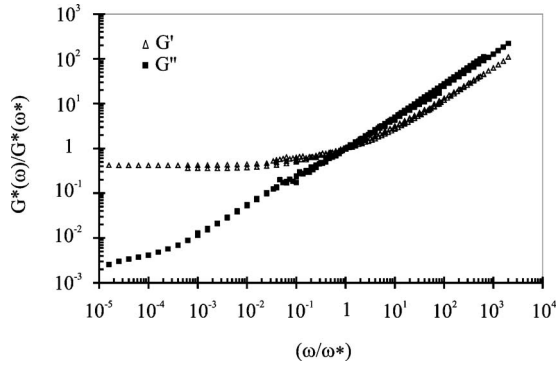


FIG. 3. Master curve of polymer 5 for  $r > r_c$ .

From the rheological curves above the gel point, one can build the master curves  $G^*(\omega)/G^*(\omega^*)$  versus  $\omega/\omega^*$  above the critical transition of polymers 5 and 6.  $\omega^*$  is defined as the frequency at which  $G' = G''$ . The master curve is obtained through eight decades for polymer 5 and six decades for polymer 6, from the viscoelastic curves corresponding to different relative distances to the threshold (Figs. 3 and 4, respectively). Getting such different master curves for polymers 5 and 6 establishes that the dynamic properties of both polymers are governed by the molecular structure of the pre-polymers and cross-linkers, the self-similarity of the structure of the incipient gel, and the self-similarity of the mass distribution of clusters.

Moreover, from the rheological curves above the gel point, one can plot  $G \propto \omega^{*u}$  for seven polymers (Fig. 5). Figure 5 allows us to obtain the same  $u$  values as found previously, independently of the  $r_c$  values but with a lower accuracy. All the  $r_c$  values have been confirmed by dissolution experiments in THF.

From the best fit of the experimental curves with relations (5) and (6), we obtain values of  $\tau_0$  between  $1.3 \times 10^{-7}$  and  $4.7 \times 10^{-8}$  s for all polymers. That means these  $u$  values were determined in a range of frequencies where  $\omega \ll \omega_0 \approx 1/\tau_0$ , where  $\omega_0$  is the internal cutoff frequency. The fractal dimension  $D_f$  can be calculated from Eq. (8). The fractal dimension obtained for polymers 1–7 varies between 1.90 and 2.35 whereas the percolation theory predicts a fractal dimension of  $D_f = 2.5$ , independently of the structure.

Table II reports the experimental values of  $r_c$ ,  $u$ , and  $D_f$ . As expected, an increase of the functionality of the cross-

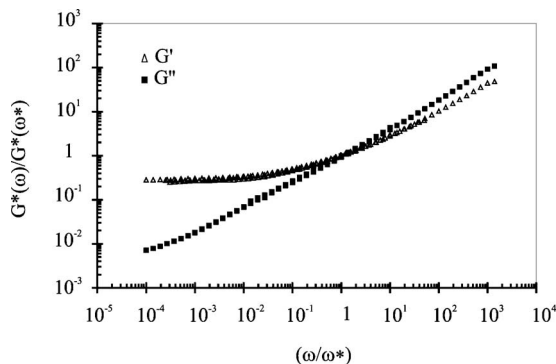


FIG. 4. Master curve of polymer 6 for  $r > r_c$ .

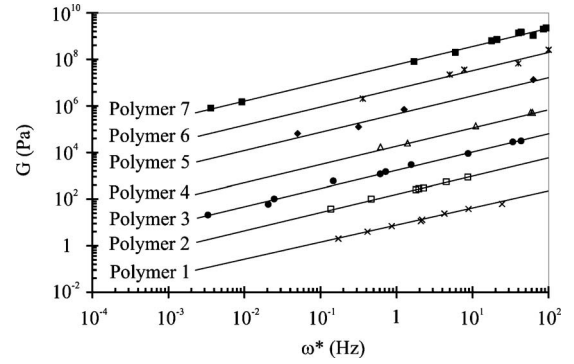


FIG. 5. Representation of the zero-frequency moduli  $G_1$ ,  $G_2 \times 50$ ,  $G_3 \times 600$ ,  $G_4 \times 10^3$ ,  $G_7 \times 10^7$  (data from Ref. [18]) and  $G_5 \times 10^4$ ,  $G_6 \times 2 \times 10^6$  versus  $\omega^*$ . From the scaling relation  $G \propto \omega^{*u}$ , we found the same values as in Table II, but with a lower accuracy ( $\pm 0.03$ ).

linker involves a decrease of the critical stoichiometric ratio. The discrepancy in the  $r_c$  values can be explained by the fact that a small variation of the molecular weight or functionality induces a significant change of the  $r_c$  value. Moreover, the theoretical  $r_c$  value can be calculated more precisely using the weight functionality of the reagents. Unfortunately, the NMR measurements used in this study give only the number functionality of reagents.

Comparison of the critical exponent  $u$  and  $D_f$  shows that for polymer 1, they are significantly different from those obtained for the other polymers.

In the literature, we found only one study by Adam *et al.* [42] which can be really compared to our seven PDMS polymers. In their work, the PDMS networks were synthesized from the TDS cross-linker and a divinyl PDMS prepolymer with  $M_n = 4900$  g/mol. The functionality and the molecular weight of the TDS were measured by gas chromatography/mass spectroscopy analysis:  $f = 3.87$  and  $M_n = 342$  g/mol. One can note that the functionality and the molecular weight of our TDS measured by NMR are slightly different and closer to those calculated from the chemical structure ( $f = 4$  and  $M_n = 328.73$  g/mol). The  $r_c$  and  $u$  values characteristic of the PDMS network of Adam *et al.* [42] are  $0.335 \pm 0.010$  and  $0.690 \pm 0.005$ , respectively.

The comparison of  $u$  and  $D_f$  first between polymers 2 and 7, and then between polymer 1 and the one of Adam *et al.* [42], shows that the molecular weight of the vinyl prepoly-

TABLE II. Critical values of polymers 1, 2, 3, 4, 5, 6, and 7.  $D_f$  is derived using Eq. (8).

Critical values	$r_c$	$u$	$D_f$
Polymer 1	$0.44 \pm 0.01$	$0.69 \pm 0.01$	$2.35 \pm 0.06$
Polymer 2	$0.26 \pm 0.01$	$0.76 \pm 0.01$	$1.95 \pm 0.05$
Polymer 3	$0.23 \pm 0.01$	$0.75 \pm 0.03$	$2.00 \pm 0.16$
Polymer 4	$0.30 \pm 0.01$	$0.77 \pm 0.01$	$1.90 \pm 0.05$
Polymer 5	$0.25 \pm 0.01$	$0.78 \pm 0.03$	$1.85 \pm 0.15$
Polymer 6	$0.21 \pm 0.01$	$0.77 \pm 0.01$	$1.90 \pm 0.05$
Polymer 7	$0.29 \pm 0.01$	$0.76 \pm 0.01$	$1.95 \pm 0.05$

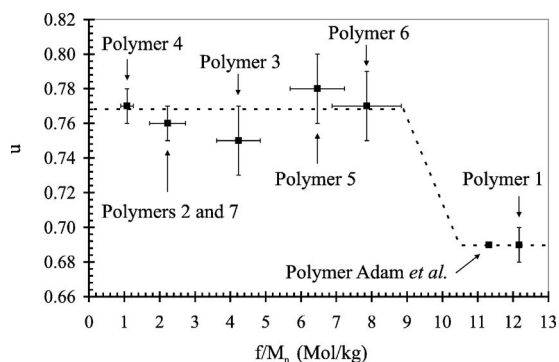


FIG. 6. Critical exponent  $u$  of polymers 1–7 and polymer of Ref [42] versus the ratio  $(f/M_n)$ , characteristic of cross-linkers.

mer does not change the fractal dimension and the rheological behavior at the sol-gel transition.

Comparison between polymers 5 and 6 shows that the structure of the cross-linker, linear or cubic, does not affect the critical viscoelastic properties; this result confirms that the relaxation times of the clusters measured in the experimental window are significantly larger than  $\tau_0$ . Then, the structural differences between polymers seem to arise mainly from the functionality  $f$  and the average molecular weight  $M_n$  of the cross-linker. According to this idea, the curves displayed in Figs. 6 and 7 show that both  $u$  and  $D_f$  present a crossover with the ratio  $f/M_n$ . The ratio  $f/M_n$  could be understood as a branching rate that governs the local fractal structure of polymers. One can analyze this result by considering that  $D_f$  of polymer 1 is close to 2.5 and  $D_f$  of polymers 2–7 ranges between 1.9 and 2 (Fig. 7). Hence, polymer 1 could arise from a critical percolation process and polymers 2–7 from a diffusion-limited cluster aggregation (DLCA) process [or other aggregation mechanisms for which  $D_f \approx 1.9$ , like reaction-limited cluster aggregation (RLCA)]. In this case,  $D_f$  is universal and is characteristic of the aggregation process, which is controlled by the structural parameters of the cross-linkers. Then, the  $u$  values measured in the frequency window depend on the structural effects on the aggregation mechanisms of the reagents. As shown by numerical simulations [15,16], as the gelation proceeds at constant  $r$ , the large clusters can be characterized by several fractal dimensions at different scales. This structural varia-

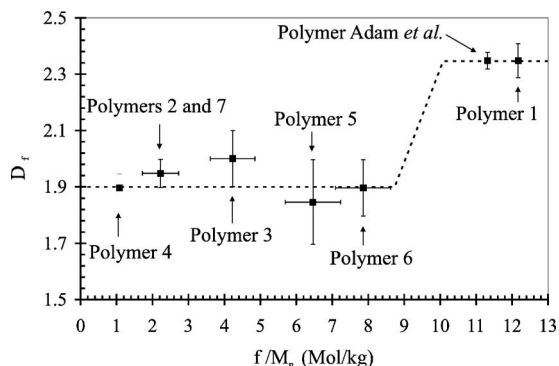


FIG. 7. Fractal dimension  $D_f$  of polymers 1–7 and polymer of Ref. [42] versus the ratio  $(f/M_n)$ , characteristic of cross-linkers.

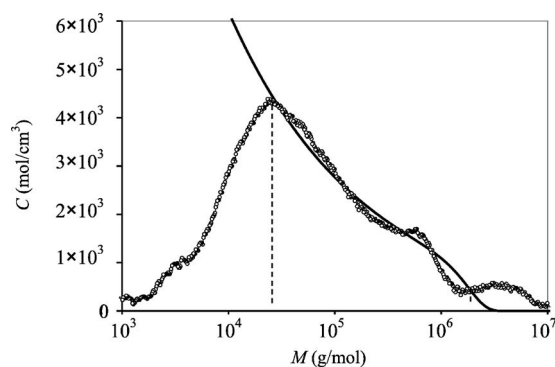


FIG. 8. Molecular weight distribution for polymer 1 around  $r_{c1} \approx 0.44$ , given in PS equivalent molecular weight. The theoretical curve (solid line) is plotted for  $\tau_1 \approx 2.3$  and  $M_{01} \approx 23500$  g/mol. An exponential function is used as a cutoff function with  $\beta=3$  [Eq. (12)].

tion results from crossovers in growth mechanism during gelation. We want to point out again that the  $u$  values measured in our experimental window are characteristic of the gel structure for a scale where the corresponding relaxation mechanisms can be observed. Thus, the DLCA is the main growth mechanism for large clusters of polymers 2–7 until the last growth stage for which the connectivity at the end of the gel growth occurs by critical percolation. On the other hand, the cluster growth mechanism of polymer 1 seems to be the critical percolation, whatever the size of the clusters is.

We wanted to check the difference between the  $D_f$  value of polymer 1 and the one of polymers 2–7. It is well known that it is impossible to measure  $D_f$  of the incipient gels in bulk. However, we are able to measure the swollen fractal dimension  $D_f^s$  for two characteristic polymers and verify if the  $D_f$  values are coherent with those of  $D_f^s$ . The two polymers chosen are polymers 1 and 2, for which  $u$  and  $D_f$  were obtained with good accuracy.

The molecular weight distributions of polymers 1 and 2 for  $r \approx r_c$  were measured by size exclusion chromatography (SEC). The chromatograms are presented in Figs. 8 and 9. One can note that polymer 2 is characterized by a molecular

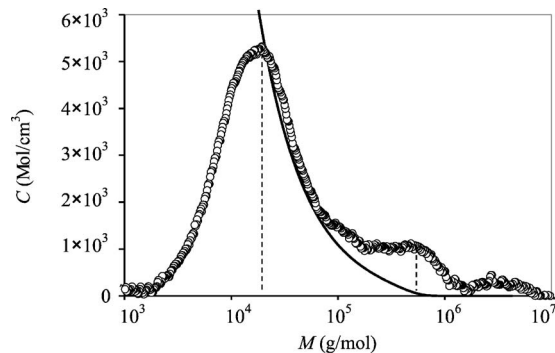


FIG. 9. Molecular weight distribution for polymer 2 around  $r_c \approx 0.26$ , given in PS equivalent molecular weight. The theoretical curve (solid line) is plotted for  $\tau_2 \approx 3$  and  $M_{02} \approx 20000$  g/mol. An exponential function is used as a cutoff function with  $\beta=3$  [Eq. (12)].

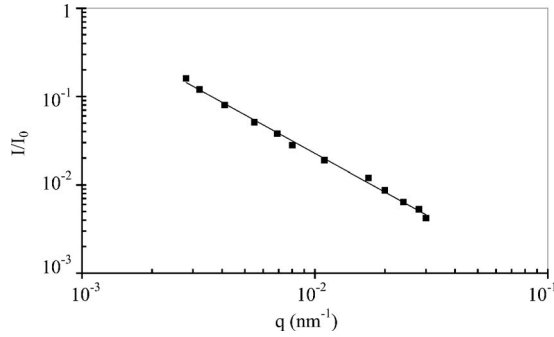


FIG. 10. Scattering wave vector dependence of the normalized intensity of polymer 1 around  $r_{c1}=0.44$  and diluted 2000 times in toluene. The slope of the solid line gives the effective fractal dimension  $D_{f1}^{eff} \approx 1.5$ .

weight distribution more narrow than the one of the polymer 1. The two chromatograms are present for the high-molecular-weight small humps due to an effect of complete elution of the largest aggregates. We do not have an explanation for these humps. Such a feature was also observed in other systems and could be an artifact of the method [43–45]. The molecular weight corresponding to the maximum of concentration is  $M_0$ ; it is the molecular weight of the smallest fractal cluster that has a relaxation time  $\tau_0$  (internal cutoff).  $M_0$  is on the same order for both polymers ( $M_0 \approx 20\,000$  g/mol in equivalent polystyrene molecular weight).  $\tau$  was obtained from the two chromatograms using relation (12). We found  $\tau_1 \approx 2.3$ , in agreement with the critical percolation theory for polymer 1 and  $\tau_2 \approx 3$  for polymer 2, which confirms that the growth mechanism for this polymer differs from the critical percolation theory. One can note that the fit for polymer 2 is not as good as expected essentially because of parasitic humps at high molecular weight. The molecular weight distribution of polymer 2 is symmetrical and does not follow the power law of relation (1). Such symmetrical distributions are also observed in the DLCA model (and was also obtained for polymer 6). The  $D_f^{eff}$  values were obtained from scattering light experiments (Figs. 10 and 11) and are around 1.5 for the two polymers. By considering the  $\tau$  values,  $D_f^s$  were calculated for each polymer:  $D_{f1}^s = 1.95$  and  $D_{f2}^s = 1.5$  for polymers 1 and 2, respectively.

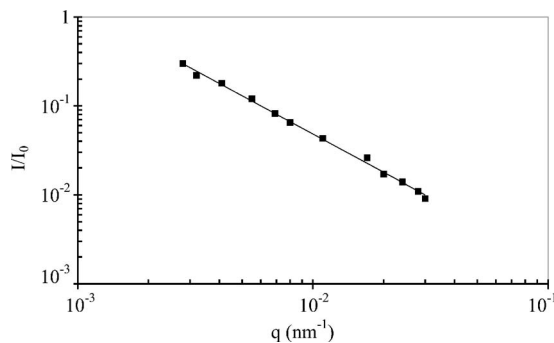


FIG. 11. Scattering wave vector dependence of the normalized intensity of polymer 2 around  $r_{c2}=0.26$  and diluted 2000 times in toluene. The slope of the solid line gives the effective fractal dimension  $D_{f2}^{eff} \approx 1.5$ .

TABLE III. Fractal dimensions in bulk  $D_f$ , swollen fractal dimensions in dilute solution  $D_f^s$ , and polydispersity exponents  $\tau$  for polymers 1 and 2.

	$D_f$	$D_f^s$	$\tau$
Polymer 1	2.35	2.14	2.3
Polymer 2	1.95	1.5	3

Comparison of  $D_f^s$  and  $D_f$  in Table III shows that  $D_f^s < D_f$  for both polymers, as expected. Moreover, the swollen or bulk fractal dimension of polymer 1 is higher than the one of polymer 2. These results are coherent together and confirm indirectly that  $D_f$  could be extracted from viscoelastic measurements using the model presented in Sec. II. Hence, the molecular structure of polymer 1 differs considerably from the one of polymer 2, generalizing, from the one of polymers 2–7. The  $D_f$  value of polymer 1 is around 2.35. The difference with the theoretical value 2.52 could be due to the fact that the hydrodynamic interactions may be not fully screened for polymer 1 (synthesized with the lowest molecular weight crosslinker).

The  $u$  exponent and the corresponding  $D_f$  were measured at  $r \approx r_c$  for the seven polymers. In all cases  $D_f < 4$ , meaning that the growth mechanisms are different from the mean field mechanism, although  $\epsilon_G$  of polymers 2–7 are lower than  $\epsilon_G$  of polymer 1 and the accuracy of the relative distance to the threshold that results from the accuracy of our balance for the experiments at  $r \approx r_c$  is lower than  $\epsilon_G$  for the seven polymers. Thus, our experimental protocol allows one to study the static and dynamic properties of gels around the threshold in the critical region.

Recently, Lusignan *et al.* [17] found, by studying a series of randomly branched polyesters, that relation (3) was valid in the mean field theory framework and then was universal. Moreover, they found that the crossover in the growth mechanisms between the critical percolation and the mean field theory occurs at  $N \approx 2N_e$ . In the mean field region,  $u$  is nonuniversal and is affected by the entanglements. Following this approach, we point out in Fig. 12 that the crossover previously observed for our series of polymers occurs at  $N \approx N_e$  ( $N_e = 44$ ) [17,46].  $N$  was calculated from Eq. (2) with  $n_0 = 2$ ,  $m_0 = 74$ , and  $C_\infty = 6$  [47]. We find from our experimental results that for  $N < N_e$ , the molecular structure of the PDMS networks around the gel point is modeled by the critical percolation theory and  $D_f$  and  $u$  are universal (2.35 and 0.69, respectively). For  $1 \leq N/N_e \leq 2$ , the growth mechanism is DLCA like and  $D_f$  and  $u$  are also universal (1.9 and 0.76, respectively). In this case, there is on average one entanglement per chain. One can think that this low number of entanglements first favors the cluster formation, following by a cluster aggregation. For  $N > 2N_e$ , as shown by Lusignan *et al.* [17], the vulcanization governs the growth of the incipient gel:  $D_f = 4$  is universal and  $u$  is a decreasing function of  $N/N_e$ . The crossover between critical percolation and DLCA in Fig. 6 seems to depend on different molecular parameters but one can demonstrate that  $(f/M_n)^{-1}$  scales as  $N [(f/M_n)^{-1} \approx Nm_0 C_\infty / n_0 - M_{vinyl}]$ , and the results are consistent.

It is important to confront these results with the literature for PDMS networks. Scanlan and Winter [13] pointed out for



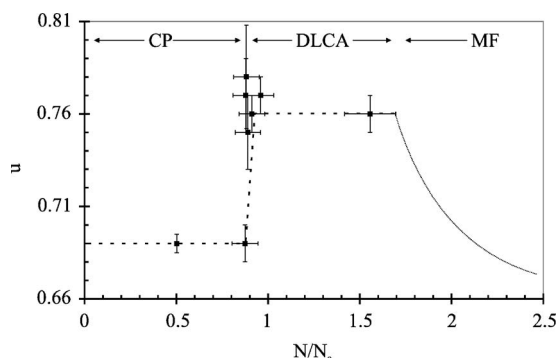


FIG. 12. Variation of the critical exponent  $u$  for the seven PDMS gels and polymer of Ref. [42] with the ratio  $N/N_e$  where  $N$  and  $N_e$  are the numbers of Kuhn monomers between branch points and between entanglements, respectively, showing three universality classes: critical percolation (CP) for  $N/N_e < 1$ , diffusion-limited cluster aggregation (DLCA) process for  $1 < N/N_e < 2$ , and mean field (MF) theory for  $N/N_e > 2$ , with regard to the results of Lusignan *et al.* [17].

PDMS gels synthesized from similar divinyl prepolymers and a 4-SiH cross-linker that  $u$  is a decreasing function of the stoichiometric ratio  $r$  and belongs to a range between 0.19 and 0.92 with an accuracy between 0.01 and 0.03 (Fig. 13). For  $r \gg r_c$ , hydrosilation reactions first lead to a formation of linear polymers entangled. Thus, the decrease of  $u$  with  $r$ , as the decrease of  $u$  with  $N/N_e$ , seems to be due to the complex effects of entanglements as proposed by Lusignan *et al.* [17].

## V. CONCLUSION

We studied the viscoelastic properties of a structural series of seven PDMS networks around the gel point. We measured the critical exponent  $u$  for all polymers at the critical stoichiometric ratio  $r_c$  and at  $r > r_c$  from the  $G(\omega^*)$  curves. On the basis of the Rouse model applied to fractal polymers, we calculated  $D_f$  for each polymer. The results show that polymer 1 is characterized by a value of  $D_f$  close to the theoretical one of critical percolation ( $D_f \approx 2.35$ ). On the other hand, polymers 2–7 present a same  $D_f$  characteristic of DLCA ( $D_f \approx 1.90$ ). We verified for polymers 1 and 2 that the  $D_f$  values obtained from viscoelastic measurements are co-

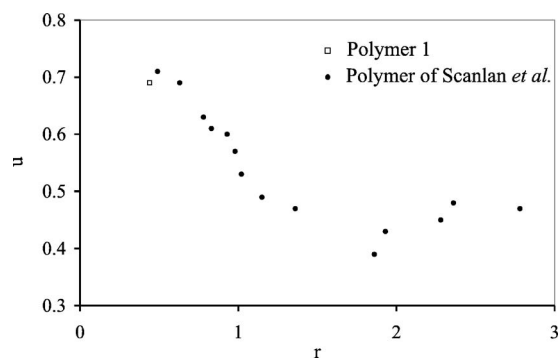


FIG. 13. Variation of the critical exponent  $u$  with the stoichiometric ratio  $r$  for the polymers of Ref. [13] and for polymer 1.

herent with the  $D_f^s$  values measured by static scattering light experiments. The analysis of these latter experiments is based on previous measurements of the polydispersity exponent  $\tau$ . SEC experiments confirm that the molecular distributions of polymers 1 and 2 are significantly different, corresponding to two different gelation mechanisms. The experimental  $\tau$  value of polymer 1 is close to 2.2, characteristic value of the critical percolation.

Our experiments point out the existence of a crossover between two universality classes: critical percolation  $N/N_e < 1$  and DLCA for  $N/N_e > 1$ . The critical percolation is observed for  $N < N_e$  when the DLCA is observed for  $N > N_e$ . Then, the percolation mechanism of PDMS gels in bulk conditions is determined by molecular parameter  $N/N_e$ . Taking the results of Lusignan *et al.* [17] and of Scanlan and Winter [13] into account, we are allowed to consider that the variation of  $u$  for a large range of  $N/N_e$  is characterized by two crossovers: for  $N/N_e < 1$ , polymer gelation is governed by critical percolation and  $u$  and  $D_f$  are universal; for  $1 < N/N_e < 2$ , gelation is governed by DLCA and  $u$  and  $D_f$  are also universal; for  $N/N_e > 2$ , gelation is governed by mean field theory,  $D_f$  is universal, and  $u$  is nonuniversal and seems to be controlled by the entanglement effects.

## ACKNOWLEDGMENTS

The authors thank J.P. Bunel for SEC experiments and especially D. Durand for fruitful discussions and static light scattering experiments.

- 
- [1] M. Adam and D. Lairez, in *Physical Properties of Polymeric Gels*, edited by J. P. Cohen Addad (Wiley, New York, 1996).  
 [2] P. de Gennes, *Scaling Concepts in Polymer Physics* (Cornell University Press, Ithaca, NY, 1979).  
 [3] D. Stauffer, A. Coniglio, and M. Adam, *Adv. Polym. Sci.* **44**, 103 (1982).  
 [4] R. Larson, *The Structure and Rheology of Complex Fluids* (Oxford University Press, Oxford, 1999).  
 [5] L. Leibler and F. Schosseler, *Phys. Rev. Lett.* **55**, 1110 (1985).  
 [6] F. Schosseler, H. Benoit, Z. Grubisic-Gallot, C. Strazielle, and L. Leibler, *Macromolecules* **22**, 400 (1989).  
 [7] D. Stauffer and A. Aharony, *Percolation theory* (Taylor & Francis, London, 1992).  
 [8] P. J. Flory, *J. Am. Chem. Soc.* **63**, 3083 (1941).  
 [9] W. H. Stockmayer, *J. Chem. Phys.* **11**, 45 (1943).  
 [10] W. H. Stockmayer, *J. Chem. Phys.* **12**, 125 (1944).  
 [11] P. J. Flory, *Principles of Polymer Chemistry* (Cornell University Press, Ithaca, NY, 1953).  
 [12] M. Daoud, *J. Phys. (Paris)* **37**, L201 (1979).  
 [13] J. C. Scanlan and H. Winter, *Macromolecules* **24**, 47 (1991).

- [14] M. Daoud and A. Lapp, *J. Phys.: Condens. Matter* **2**, 4021 (1990).
- [15] M. Rottereau, J. C. Gimel, T. Nicolai, and D. Durand, *Eur. Phys. J. E* **15**, 133 (2004).
- [16] M. Rottereau, J. C. Gimel, T. Nicolai, and D. Durand, *Eur. Phys. J. E* **15**, 141 (2004).
- [17] C. P. Lusignan, T. H. Mourey, J. C. Wilson, and R. H. Colby, *Phys. Rev. E* **60**, 5657 (1999).
- [18] T. Tixier, Ph. Tordjeman, G. Cohen-Solal, and P. H. Mutin, *J. Rheol.* **48**, 39 (2004).
- [19] Ph. Tordjeman, C. Fargette, and P. H. Mutin, *J. Rheol.* **45**, 995 (2001).
- [20] M. Cates, *J. Phys. (Paris)* **46**, 1059 (1985).
- [21] D. M. Sunell Buzza, D. J. Groves, T. C. B. McLeish, D. Parker, A. J. Keeney, and W. J. Feast, *Macromolecules* **35**, 9605 (2002).
- [22] P. J. de Gennes, *J. Phys. (France) Lett.* **38**, L355 (1977).
- [23] F. Chambon and H. Winter, *Polym. Bull. (Berlin)* **13**, 683 (1985).
- [24] D. Durand, M. Delsanti, M. Adam, and J. Luck, *Europhys. Lett.* **3**, 297 (1987).
- [25] M. Rubinstein, R. Colby, and J. Gillmor, *Polym. Prepr. (Am. Chem. Soc. Div. Polym. Chem.)* **30**, 81 (1989).
- [26] M. A. V. Axelos and M. Kolb, *Phys. Rev. Lett.* **64**, 1457 (1990).
- [27] D. Lairez, M. Adam, E. Raspaud, J. Emery, and D. Durand, *Prog. Colloid Polym. Sci.* **90**, 37 (1992).
- [28] J. E. Martin, D. Adolf, and J. P. Wilcoxon, *Phys. Rev. Lett.* **61**, 2620 (1988).
- [29] J. E. Martin, D. Adolf, and J. P. Wilcoxon, *Phys. Rev. A* **39**, 1325 (1989).
- [30] M. Muthukumar, *J. Chem. Phys.* **83**, 3161 (1985).
- [31] M. Muthukumar, *Macromolecules* **22**, 4656 (1989).
- [32] F. Chambon and H. Winter, *J. Rheol.* **31**, 683 (1987).
- [33] T. Nicolai, H. Randrianantoandro, F. Prochazka, and D. Durand, *Macromolecules* **30**, 5897 (1997).
- [34] E. Williams, J. Wengrovius, V. Valkenburgh, and J. Smith, *Macromolecules* **24**, 1445 (1991).
- [35] M. Gottlieb, C. Macosko, G. Benjamin, K. Meyers, and E. Merrill, *Macromolecules* **14**, 1039 (1981).
- [36] S. K. Venkataraman, L. Coyne, F. Chambon, M. Gottlieb, and H. Winter, *Polymer* **30**, 2222 (1989).
- [37] T. H. Mourey and S. T. Balke, *ASC Symp. Ser.* **521**, 180 (1993).
- [38] F. Prochazka, T. Nicolai, and D. Durand, *Macromolecules* **33**, 1703 (2000).
- [39] C. Degoulet, T. Nicolai, D. Durand, and J. P. Busnel, *Macromolecules* **28**, 6819 (1995).
- [40] J. E. Martin and B. J. Ackerson, *Phys. Rev. A* **31**, 1180 (1985).
- [41] T. Nicolai, D. Durand, and J. C. Gimel, *Phys. Rev. B* **50**, 16357 (1994).
- [42] M. Adam, D. Lairez, M. Karpasas, and M. Gottlieb, *Macromolecules* **30**, 5920 (1997).
- [43] V. Lesturgeon, D. Durand, and T. Nicolai, *Eur. Phys. J. B* **9**, 83 (1999).
- [44] E. V. Patton, J. A. Wesson, M. Rubenstein, J. C. Wilson, and L. E. Oppenheimer, *Macromolecules* **22**, 1946 (1989).
- [45] F. Schosseler, M. Daoud, and L. Leibler, *J. Phys. (Paris)* **51**, 2373 (1990).
- [46] C. P. Lusignan, Ph.D. thesis, University of Rochester, 1996.
- [47] *Polymer Handbook*, 4th ed., edited by J. Brandrup, E. H. Immergut, and E. A. Grulke (Wiley, New York, 1999).